Kinetic properties of the acylneuraminate cytidylyltransferase from *Pasteurella haemolytica* A2[1]

Ignacio G. BRAVO, Sofía BARRALLO, Miguel A. FERRERO, Leandro B. RODRÍGUEZ-APARICIO, Honorina MARTÍNEZ-BLANCO and Ángel REGLERO[2]

Departamento de Bioquímica y Biología Molecular, Universidad de León, Campus Vegazana, 24071 León, Spain

Neuroinvasive and septicaemia-causing pathogens often display a polysialic acid capsule that is involved in invasive behaviour. *N*-Acetylneuraminic acid (NeuAc) is the basic monomer of polysialic acid. The activated form, CMP-Neu5Ac, is synthesized by the acylneuraminate cytidylyltransferase (ACT; EC 2.7.7.43). We have purified this enzyme from *Pasteurella haemolytica* A2 to apparent homogeneity (522-fold). The protein behaved homogeneously on SDS/PAGE as a 43 kDa band, a size similar to that of *Escherichia coli*, calf, mouse and rat. Specific activity in crude lysate displayed one of the highest values cited in the literature (153 m-units/mg). We have studied the steady-state kinetic mechanism of the enzyme by using normalized plot premises. The catalysis proceeds through a Ping Pong Bi Bi mechanism, with CTP as the first substrate and CMP-NeuAc as the last product. The true K_m values were 1.77 mM for CTP and 1.82 mM for NeuAc. The nucleotides CDP, UTP, UDP and TTP, and the modified sialic acid *N*-glycolylneuraminic acid were also substrates of the ACT activity. The enzyme is inhibited by cytidine nucleotides through binding to a second cytidyl-binding site. This inhibition is greater with nucleotides that display a long phosphate tail, and the genuine inhibitor is the substrate CTP. At physiological concentrations, ATP is an activator, and AMP an inhibitor, of the ACT activity. The activated sugar UDP-*N*-acetylglucosamine acts as an inhibitor, thus suggesting cross-regulation of the peptidoglycan and polysialic acid pathways. Our findings provide new mechanistic insights into the nature of sialic acid activation and suggest new targets for the approach to the pathogenesis of encapsulated bacteria.

Key words: *N*-acetylneuraminic acid, CMP-Neu5Ac synthetase, glycobiology, sialic acids.

INTRODUCTION

Pasteurella haemolytica is a small, non-motile, encapsulated Gram-negative coccobacillus. Two biotypes (A and T) can be distinguished according to their biochemical and clinical differences, and both biotypes are subdivided into different serotypes [1–3]. Different strains of this bacterium are able to cause meningitis, localized infections, abortions and mastitis in cattle and sheep [4]. *P. haemolytica* A2 is present in the nasopharynx of healthy animals, and is the most important pathogenic agent involved in losses due to pneumonic pasteurellosis [1].

P. haemolytica A2 is known to produce a capsule whose structure is a homopolymer of α-D-*N*-acetylneuraminic acid (NeuAc) linked NeuAcα2–8NeuAc [5]. This polymer is called polysialic acid or colominic acid and is chemically identical with the capsular polysaccharides of the human meningitis-causing organisms *Neisseria meningitidis* B and *Escherichia coli* K1 [6, 7]. This outer structure resembles the glycidic fraction of many host glycoproteins. Its presence could account for the immunotolerance and virulence of infections, avoiding complement fixation and phagocytosis [8]. The negative surface charge conferred by the polymer precludes activation of host defence mechanisms [9]. The similarities between these polysaccharide structures in different micro-organisms may be accounted for in terms of convergent evolution and/or horizontal transmission of genetic information [5]. Because of the economic and clinical importance of these defensive mechanisms, in both humans and animals, elucidation of therapeutic targets is important. No effective vaccines have been developed for these diseases, and the synthesis pathway, export and genetic regulation of capsular polysaccharides have been proposed as such targets [10].

In bacteria, the biosynthesis of sialic acid begins with epimerization of *N*-acetylglucosamine 6-phosphate (GlcNAc-6-*P*) into *N*-acetylmannosamine 6-phosphate (ManNAc-6-*P*), catalysed by GlcNAc-6-*P* epimerase (EC 5.1.3.9) [11]. This enzyme branches from the common metabolism of amino sugars and regulates the amount of substrate driven into the synthesis of sialic acid, since GlcNAc-6-*P* is also involved in other capsular structures, such as peptidoglycan [12,13]. In bacteria, ManNAc-6-*P* is dephosphorylated prior to condensation with either phosphoenolpyruvate (PEP) or pyruvate (Pyr), catalysed by NeuAc lyase or synthase (EC 4.1.3.19), in both cases resulting in the production of NeuAc [7,14–17].

The biosynthesis of NeuAc follows a different pathway in mammals than in bacteria, but both systems converge in the activation step of the monomer, and the basic monomer of sialylated structures is NeuAc in both mammals and bacteria. Prior to its incorporation into biological structures, NeuAc must be activated to CMP-NeuAc by acylneuraminate cytidylyltransferase (ACT; EC 2.7.7.43) [18]. This is the sugar-nucleotide

Abbreviations used: ACT, acylneuraminate cytidylyltransferase; BHIB, Brain Heart Infusion Broth; CMP-NeuAc, CMP-*N*-acetylneuraminic acid; CMP-NeuGc, CMP-*N*-glycolylneuraminic acid; Nbs_2 ('DTNB'), 5,5′-dithiobis-(2-nitrobenzoic acid); DTT, dithiothreitol; ManNAc, *N*-acetylmannosamine; -6-*P*, 6-phosphate; NeuAc, *N*-acetylneuraminic acid; NeuGc, *N*-glycolylneuraminic acid; PEP, phosphoenolpyruvate; PHMB, *p*-hydroxymercuribenzoic acid; Pyr, pyruvate; UDP-GlcNAc, UDP-*N*-acetylglucosamine.

[1] This paper is dedicated to Professor J. A. Cabezas on the occasion of his retirement.

[2] To whom correspondence should be addressed (e-mail dbbarc@isidoro.unileon.es).

donor form used by sialyltransferase during assembly into the polymer. ACTs have been purified and the encoding genes cloned from bacterial and animal sources: *E. coli* [19,20], *N. meningitidis* [16,21], *Streptococcus agalactie* [22,23], *Haemophilus ducreyi* [24], rat liver [25], Chinese-hamster ovary cells [26,27] and bovine anterior pituitary glands [28]. The catalytic reaction is specific for the β-anomer conformation on the C-2 hydroxy group of NeuAc and results in the formation of CMP-β-NeuAc [29] through an ordered Bi Bi mechanism, with CTP binding first and CMP-NeuAc dissociating last [30]. The enzyme has been crystallized as a dimer from *N. meningitidis*, and a conformational change in the presence of CDP has been reported, supporting the proposed order of substrate binding [31].

Here we detail study of the kinetic properties of the ACT from *P. haemolytica* A2 with the aim of gaining new insights into pathogenic encapsulated bacteria and prophylaxis of the diseases they are responsible for.

MATERIALS AND METHODS

Chemicals

[*Neu*-4,5,6,7,8,9-^{14}C]NeuAc (300 Ci/mol) and CMP-[*Neu*-4,5,6,7,8,9-^{14}C]NeuAc (267 Ci/mol), Butyl-Sepharose fast flow, Superdex S-200, Sephadex G-25 and molecular-mass markers were purchased from Amersham International. Borohydride, mercaptoethanol, 5,5′-dithiobis-(2-nitrobenzoic acid) (Nbs_2) and *p*-hydroxymercuribenzoic acid (PHMB) were purchased from Merck. *N*-Ethylmaleimide was from BDH Laboratory Reagents. Matrex Gel Red A was purchased from Amicon. Brain Heart Infusion Broth (BHIB) and Brain Heart Infusion Agar were from Pronadisa (Madrid, Spain). All other reagents were purchased from Sigma Chemical Co.

Growth of bacteria

P. haemolytica A2 (A. T. C. C. 29694) obtained from the Colección Española de Cultivos Tipo (C. E. C. T. 924) was recovered from lyophilizates as described [32], and stored in 50 % (v/v) glycerol at −70 °C. Cells were grown overnight at 37 °C in Brain Heart Infusion Agar tubes and resuspended in sterile water. For purification studies, 2-litre flasks containing 400 ml of BHIB were inoculated with 8 ml of the resuspension [attenuance (D_{540}) = 1.0]. Cultures were grown at 37 °C and 200 rev./min in a rotary shaker and collected by centrifugation (see below) after 5 h, the time when ACT activity has been found to be maximal [33].

Purification of ACT

All procedures were carried out at 4 °C, and all chromatography steps were performed on a Waters FPLC system. Column fractions were assayed for ACT activity and protein concentration. All enzyme assays were within the linear range of ACT behaviour.

Step 1: cell lysis and membrane removal

Bacteria were harvested by centrifugation at 10000 ***g*** for 10 min, washed twice in 50 mM Tris/HCl, pH 8.0, containing 25 mM $MgCl_2$ and 1.0 mM dithiothreitol (DTT), and suspended in 100 ml of the same buffer. Cells were lysed mechanically with glass beads (0.17–0.18 mm diameter) under refrigeration. Non-lysed cells were removed by centrifugation at 10000 ***g*** for 10 min. Membranes were eliminated by ultracentrifugation at 400000 ***g*** for 12 min.

Step 2: nucleic acid precipitation

Streptomycin sulphate was added at 0.75 % (w/v), the mixture stirred for 30 min and nucleic acids removed after precipitation at 37000 ***g*** for 15 min.

Step 3: $(NH_4)_2SO_4$ fractionation

The supernatant was adjusted to 45 % $(NH_4)_2SO_4$ saturation at 4 °C. The precipitate was removed after centrifugation at 37000 ***g*** for 15 min. The supernatant was then adjusted to 70 % $(NH_4)_2SO_4$ saturation and centrifuged at 37000 ***g*** for 15 min.

Step 4: hydrophobic chromatography

The pellet containing ACT was resuspended in 50 mM Tris/HCl/25 % $(NH_4)_2SO_4$, pH 7.5 (buffer A). Hydrophobic chromatography was carried out in a Butyl-Sepharose fast flow column (200 ml; 90 μm mean particle size) equilibrated in buffer A. The active suspension was applied to the column and this was washed extensively with buffer A. Elution was accomplished with a 120-min, 3 ml/min, linear gradient from buffer A to 50 mM Tris/HCl, pH 7.5 (buffer B). The fractions displaying maximum ACT activity corresponded to elution volumes ranging between 240 and 270 ml. The active fractions were pooled, adjusted to 90 % $(NH_4)_2SO_4$ saturation, and centrifuged at 37000 ***g*** for 15 min. The precipitate was resuspended in buffer B and desalted through a Sephadex G-25 (PD-10) column equilibrated in the same buffer.

Step 5: dye–ligand chromatography

Active fractions were applied to a Matrex Red A dye–ligand chromatography column (5 ml), equilibrated in buffer B. Activity was eluted by shifting from buffer B to 50 mM Tris/HCl, pH 8.5 (buffer C) at a 2 ml/min flow rate.

Step 6: anion-exchange chromatography on DEAE-Sephacel

Active fractions were pooled and applied to a DEAE-Sephacel column (10 ml; 8 μm mean particle size) equilibrated with buffer C and extensively washed with buffer B prior to elution with a 30-min, 1 ml/min, linear gradient from buffer B to 50 mM Tris/HCl/0.146 M KCl, pH 7.5. The active fractions containing purified enzyme corresponded to elution volumes ranging between 35 and 36.5 ml (the delay was attributable to the void volume in the system). These fractions were used for physicochemical characterization of the enzyme.

Amino acid analysis and N-terminal sequencing

Active fractions eluted from the DEAE column were freeze-dried, resuspended in water, and applied to a C_4 Vydac reverse-phase HPLC column equilibrated with trifluoroacetic acid/water (0.1:99.9, v/v). Elution was performed with a 45-ml, 1 ml/min, linear gradient from this solution to trifluoroacetic acid/water/acetonitrile (0.1:4.9:95, by vol.). The peak co-migrating with the purified enzyme in SDS/PAGE was sequenced by Edman degradation. Amino acid analysis was carried out using the standardized Waters AccQ-Tag method. Derivatized amino acids were separated in a Waters Pico-Tag system.

ACT assay

The reaction mixture, with a final volume of 125 μl, contained 17.5 μl of active extract (approx. 0.20 μg of protein/ml) and final concentrations of 5.0 mM CTP, 5.0 mM NeuAc, 10 mM $MgCl_2$, 5.0 mM DTT and 180 mM Tris/HCl, pH 9.0. The mixture was

incubated at 37 °C for 30 min and the reaction was stopped by cooling the sample in ice/water. ACT activity was measured using three different procedures, depending on the specific characteristics of each assay. Colorimetric quantification of CMP-NeuAc production was the preferred scheme. This was carried out following the original method of Kean and Roseman [34], as modified by Rodríguez-Aparicio et al. [35]. When the reaction mixture contained molecules that interfered with the resorcinol method, such as adenine or guanidine derivatives, either a radiometric or an enzymic determination of PP_i was used. Radiometric quantification of CMP-NeuAc after paper chromatography was carried out as described by Rodríguez-Aparicio et al. [35]. The amount of released PP_i, the other product of ACT activity in the anabolic sense, was determined by a coupled enzymic assay; 2 mol of NADH are oxidized to NAD^+/mol of pyrophosphate (PP_i) consumed, as described by O'Brien [36].

In all cases, calibration of the method was performed with commercial NeuAc as standard. One unit of enzyme is described as the amount of enzyme capable of producing 1 μmol of CMP-NeuAc/min. Protein was determined by the Bradford method [37], according to the manufacturer's (Bio-Rad) instructions, using BSA as protein standard.

Characterization of ACT

Dependence on cations, pH and redox conditions

To determine optimal pH, 180 mM potassium phosphate buffer in the range pH 6.5–8.0, 180 mM Tris/HCl in the range 7.5–9.5 pH, 180 mM glycine/NaOH in the range pH 8.5–10.0 or 180 mM Tris/NaOH in the range pH 10.5–12.5 were used. To elucidate ion requirements, 10 mM chloride salts of the following cations were used: Na^+, K^+, Rb^+, Li^+, Cs^+, Ca^{2+}, Ni^{2+}, Sr^{2+}, Mn^{2+}, Co^{2+}, Hg^{2+}, Cu^{2+} Ba^{2+}, Zn^{2+} and Fe^{3+}. $MgCl_2$ and $MnCl_2$ were also tested in the 0–100 mM range. To determine the effect of protection and modification of thiol groups on enzyme activity, the following products were tested at 1.0 mM and 5.0 mM final concentration in the reaction mixture: DTT, mercaptoethanol, *N*-ethylmaleimide, Nbs_2 and PHMB. No DTT was added to the standard reaction mixture when testing these compounds.

Determination of kinetic parameters

The experiments were designed according to normalized plot premises for kinetic determinations (see the accompanying paper [37a]). For both substrates, CTP and NeuAc, the reference concentration was 0.50 mM. Therefore, values for a (and b) refer to a (or b) times 0.50 mM. CTP was called substrate A, and NeuAc substrate B. Three experimental series were prepared: (1) $a = b$, with the concentrations of both substrates in the 0.50 mM ($a = b = 1$) and 50 mM ($a = b = 100$) range; (2) $a = 1$, keeping the CTP concentration constant at 0.50 mM and varying the NeuAc concentration between 0.50 mM ($b = 1$) and 50 mM ($b = 100$); (3) $b = 1$, keeping the NeuAc concentration constant at 0.50 mM and varying the CTP concentration between 0.50 mM ($a = 1$) and 50 mM ($a = 100$). Each experimental series involved ten values. The same procedure was followed when testing other substrates: CDP, UTP, UDP and TTP as nucleotides, and *N*-glycolylneuraminic acid (NeuGc) and NeuAc methyl ester as sugars. In the presence of the product PP_i, five sets of experiments were performed, with PP_i concentrations at 1.0, 2.5, 5.0, 10 and 20 mM. No precipitate of magnesium pyrophosphate was detected under the experimental conditions. In the presence of the product CMP-NeuAc, three sets of experiments were performed, with CMP-NeuAc concentrations at 1.0, 5.0 and 10 mM. The inhibitor CMP was tested at four concentrations: 5.0, 10, 20 and 50 mM. Cytidine was tested as an inhibitor at five concentrations: 5.0, 10, 20, 40 and 60 mM. The inhibitor UMP was tested at two concentrations: 1.0 and 10 mM. UDP-GlcNAc was tested as an effector of the enzyme at three concentrations: 1.0, 5.0 and 10 mM. ATP and AMP were tested as effectors of the activity at 1.0, 5.0 and 10 mM. GTP was tested as an effector at 10 and 1.0 mM. GMP was tested as an effector at 1.0, 5.0, 10 and 20 mM. The action of all effectors and inhibitors was tested on the three experimental series $a = b$, $a = 1$ and $b = 1$, varying the CTP and NeuAc concentrations from 0.50 to 30 mM.

Determination of molecular mass and aggregation states

SDS/PAGE was performed using 12% acrylamide. Size-exclusion chromatography of active native, partially and totally purified enzyme was carried out in a Superdex S-200 column.

Data analysis and choice among rival models

The equations that describe the behaviour of the system, and the statistical criteria used to discern among rival models, are described in the Appendix.

RESULTS AND DISCUSSION

Activity in the cell crude lysate

Bacteria were cultured in medium and conditions reported to maximize colominic acid biosynthesis by *P. haemolytica* A2 [32]. Under these conditions, the ACT from *P. haemolytica* A2 displayed one of the highest specific activities (145 m-units/mg) in cell lysates among all wild-type and genetically modified organisms reported. Only *E. coli* has been shown to produce up to 250 m-units/mg of protein (see Table 1) [38]. Thus *P. haemolytica* A2 could be an excellent target for studying and optimizing the fermentative production of ACT for use in large-scale CMP-NeuAc synthesis. This proposed optimization could probably be improved attending not only to nutritional requirements but also to the control of the temperature of growth, since it has been reported that the enzymes involved in colominic acid biosynthesis in *P. haemolytica* A2 are under temperature control, their expression being arrested when bacteria are grown above 43 °C [33].

Purification and identification of the enzyme

Purified enzyme appeared as a single 43 kDa band on SDS/PAGE and behaved homogeneously in reverse-phase HPLC. Size-exclusion chromatography afforded a molecular mass of 135 ± 12 kDa in buffer A, the functional enzyme therefore appearing to exist as a trimer. A comparative overview of the published aggregation characteristics of ATCs is shown in Table 1.

Active fractions eluted from the DEAE-Sephacel column containing purified enzyme were repurified by reverse-phase HPLC. One major peak was detected, corresponding to a protein that co-migrated with purified active enzyme in SDS/PAGE. This protein was used for N-terminal sequencing and total amino acid analysis. Edman degradation afforded a 20-amino-acid sequence with a high degree of confidence: MKKIAIITARAGSKGLPNKN. The sequence showed a high degree of similarity with the enzyme obtained from both bacterial and mammalian sources, and corresponds to a region identified as the phosphate-binding loop in the structure of the only crystallized ACT [31]. The alignment is shown in Table 2.

Table 1 Comparison of properties of ACT obtained from different sources

Source	Molecular mass (Da)	Aggregation	Activity in cell lysate (μmol/min per mg)	K_m (mM)		CTP inhibition	Use of NeuGc as substrate	References
				CTP	NeuAc			
E. coli	49000 (a)	Dimer (a)	250 (b)	8.5 (c)	4.0 (c)	–	No	(a) [20]; (b) [38]; (c) [19]
N. meningitidis B	24800 (d)	Dimer (d,e)	0.994 (d)	0.56 (f)	0.25 (f)	–	No	(d) [21]; (e) [31]; (f) [16]
S. agalactie	45500 (g)	Dimer (h)	0.004 (h)	1.4 (h)	7.6 (h)	–	–	(g) [23]; (h) [22]
H. ducreyi	25400 (i)	Dimer/higher (i)	4.74 (i)	0.0106 (j)	0.0763 (j)	Yes (j)	Yes (j)	(i) [24]; (j) [30]
P. haemolytica A2	43000	Trimer	153	1.77	1.82	Yes	Yes	The present paper
Rat liver	58000 (k)	Dimer (k)	0.008 (k)	1.5 (k)	1.3 (k)	Yes (k)	Yes (k)	(k) [25]
Mouse ovary	50000 (l)	Trimer (l)	0.00198 (l)	–	–	–	–	(l) [26]
Bovine tissues	52000 (m)	Trimer (m)	0.001 (m)	1.35 (n)	1.84 (n)	Yes (n)	Yes (n)	(m) [28]; (n) [46]

Table 2 Alignment of the N-terminal conserved domain of ACTs and comparison with 3-deoxymanno-octulosonate cytidylyltransferases

Degrees of similarity are given in decreasing order as (*, :, .). The accession number of the sequence is also given.

(a) 3-Deoxymanno-octulosonate cytidylyltransferases

Species	Degree of similarity ...	: : : * ** : : *	Accession no.
H. influenzae		--SFTVIIPA**R**FA**S**SRLPG**K**P--------	P44490
C. trachomatis		-----GILPS**R**WG**S**SRFPG**K**P--------	Q59320
E. coli		-SKAVIVIPA**R**YG**S**SRLPG**K**P--------	P42215
A. aeolicus		--RRAVIIPA**R**LG**S**TRLKE**K**P--------	O66914

(b) ACTs

Species	Degree of similarity ...	: . : : ** . ** : **	Accession no.
N. meningitidis		---N**I**AVIL**AR**QN**SK**GLPL**KN**--------	X78068
Mouse		--HLAALVL**AR**GG**SK**GIPL**KN**--------	AJ006125
H. pylori		--RA**I**AIVL**AR**SS**SK**RIKN**KN**--------	AE000550
E. coli		-TKI**I**AIIP**AR**SG**SK**GLRN**KN**--------	P13266
S. agalactie		--KP**I**CIIP**AR**SG**SK**GLPD**KN**--------	U19899
P. haemolytica		--KK**I**AIIT**AR**AG**SK**GLPN**KN**--------	
H. influenzae		--TR**I**AIIP**AR**AG**SK**GIKD**KN**--------	U32807
H. ducreyi		--KK**I**AIIP**AR**AG**SK**GIKD**KN**--------	U54496
A. caviae		---N**I**AIIP**AR**GG**SK**RIPR**KN**--------	AAD45658

There are practically no negative charges at the N-terminal domain of these enzymes; there is only one glutamate residue at position 2 in *N. meningitidis*. The hydrophobic residues isoleucine-4 and alanine-9, hydrophobic consensus at positions 5, 6, 7 and 16, serine-13, and positive charges at arginine-10, lysine-14, lysine-19 and asparagine-20 (positions in the enzyme from *P. haemolytica* A2) are conserved throughout the nine sequences in the databases. In particular, lysine-19 and arginine-12 have been shown to be located at the CTP-binding site of *E. coli* ACT [39, 40]. The common feature is arranged as a hydrophobic box followed by a positively charged box. Accordingly, these proteins do not contain the HiGH motif involved in nucleotide binding in the so-called cytidylyltransferase superfamily, which relates this superfamily to class I tRNA synthetases [41].

ACTs display close similarity to 3-deoxymanno-octulosonate cytidylyltransferase (EC 2.7.7.38) (Table 2). This enzyme catalyses the formation of CMP-3-deoxymanno-octulosonate with a concomitant release of pyrophosphate [42,43]. The parallelism between both activities is therefore obvious. Accordingly, differences and similarities in sequences are highly informative, since they point to differential physiological behaviour. The hydrophobic box, polarity at serine-13 and positive charges at arginine-10 and lysine-19 are conserved along both protein families. This conserved structure contains the lysine residue involved in CTP-binding activity and could be the general substrate-binding motif [31]. Furthermore, conserved positive charges at lysine-14 and asparagine-20 are not present in 3-deoxymanno-octulosonate cytidylyltransferase, and a conserved proline residue substitutes the former. Similarities in sequence can also be established downstream from this box, as described in [24,26].

Properties of the enzyme

The ACT from *P. haemolytica* A2 displays maximum specific activity at pH 9.0. The enzyme activity decreased dramatically below pH 7.0 and above pH 12.5. Other enzymes show maximum activity over the same pH range (*E. coli*, *Streptococcus* sp., *N. meningitidis*, *H. ducreyi*, rat liver), and ACTs from other sources have commonly been assayed in the range pH 8.0–9.0 (mouse, bovine pituitary gland) [16,19,21–28,34].

A bivalent cation is strictly required for enzyme activity. Maximum activity was detected at 10 mM Mg^{2+}, decreasing at higher Mg^{2+} concentrations. Only Mn^{2+}, Co^{2+} and Ca^{2+} were partially able to substitute Mg^{2+} in catalysis, yielding maximum activity percentages of 28, 27 and 13 % respectively when assayed at 20 mM. Increasing Mn^{2+} concentration up to 30 mM caused reversible inhibition of ACT activity. The univalent cations Na^+, K^+, Rb^+, NH_4^+, Li^+ and Cs^+ did not significantly inhibit the activity. The bivalent cations Sr^{2+} and Ba^{2+} caused less than 30 % of inhibition. By contrast, Co^{2+} inhibited ACT activity by more than 70 %, and Ca^{2+}, Mn^{2+}, Hg^{2+}, Cu^{2+}, Zn^{2+}, Fe^{3+} and Ni^{2+}

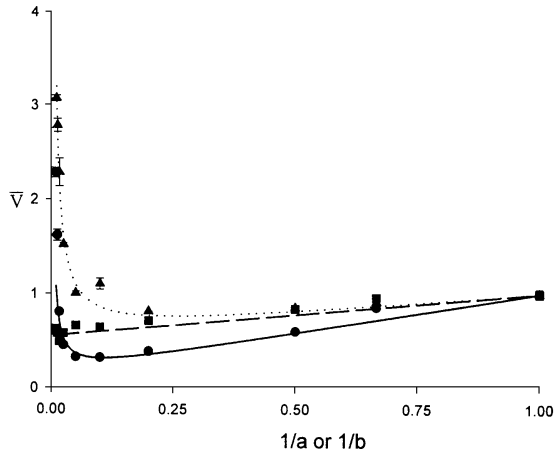

Figure 1 Plot of $\overline{V}$ against 1/*a* or 1/*b* in the absence of products for the ACT from *P. haemolytica* A2

The three experimental series are depicted: $a = b$ (●, continuous line), $a = 1$ (■, broken line) and $b = 1$ (▲, dotted line). The reference concentration was 0.5 mM for both substrates. Error bars represent S.E.M. Lines were generated using constants obtained from non-linear fit of the data to eqn (A1), for a Ping Pong Bi Bi system inhibited by substrate A (CTP) in the forms F and [FB + EQ] of the enzyme.

caused more than 90 % inhibition. All cations were assayed as 20 mM chloride under standard assay conditions containing 10 mM Mg^{2+}.

No enhancement of activity was detected when the reducing agents DTT, GSH or mercaptoethanol were used. Nevertheless, DTT was included in reaction mixture because of its stabilizing effect on protein homogenates. The thiol-modifying agent PHMB completely inhibited activity when present at 1.0 mM under optimal assay conditions. Other compounds with similar modification activity, such as Nbs_2 and *N*-ethylmaleimide, also inhibited ACT activity in a concentration-dependent fashion (results not shown). This, together with the effect of the heavy atoms Hg^{2+}, Cu^{2+} and Zn^{2+} on enzyme activity, accounts for the involvement of thiol groups in enzyme activity.

Kinetic initial data in the absence of products

Three experimental data series were generated according to normalized plot premises. Each experimental series was constructed from ten data points. The reference concentration for both substrates was 0.50 mM, and their concentrations were varied from 0.50 mM to 50 mM. Normalized velocities were plotted against normalized substrate concentrations. CTP was an inhibitor of the ACT activity and yielded a hyperbolic decay-like shape in both the $a = b$ and $a = 1$ series as a increased (Figure 1). This behaviour corresponds to one of the following situations in a Bi Bi system (see the Appendix):

(1) Ping Pong systems

(i) Substrate B is an inhibitor that binds E

(ii) Substrate A or B is an inhibitor that binds either [EA + FP] or [FB + EQ]

(2) Ordered systems

(i) Substrate A or B is an inhibitor that binds [EAB + FPQ]

(ii) Substrate A or B is an inhibitor that binds EQ

F denotes a substituted-enzyme intermediate in a Ping Pong system or a ternary complex in an ordered system.

Table 3 Election of the kinetic mechanism of the ACT from *P. haemolytica* A2

Data correspond respectively to residual sum of squares in the absence of products and different substrate couples and in the presence of the physiological substrates and of the product PP_i. Families of mechanisms are described in the text. Each value is the mean for four experiments. Abbreviation: ME, methyl ester.

		Family A				Family A						
Substrates	Number of parameters …	4	3	4	5	2	3	4	5	8	Number of data
		Family A	Family B	Family C	Family D	Ping Pong; no inhibition	Ordered; no inhibition	Ping Pong Theorell–Chance (inhibition by A on F and [FB + EQ])	Ping Pong (inhibition by A on F and [FB + EQ])	Ping Pong (inhibition by A on [EA + FP] and F)	
CTP/NeuAc		0.17665	1.03186	0.97027	0.97075	–	–				30
CTP/NeuAc ME		0.06062	0.07206	0.08068	0.06018	–	–				14
CTP/NeuGc		0.00817	0.01618	0.01481	0.00817	–	–				17
CDP/NeuAc		1.25660	2.65542	93.56317	2.25106	–	–				21
UTP/NeuAc		–	–	–	–	0.12857	0.12857				14
TTP/NeuAc		–	–	–	–	0.03010	0.03009				16
UDP/NeuAc		–	–	–	–	0.12354	0.12353				16
Product PP_i								0.51861	0.44223	3.7283	66

Table 4 Kinetic constants of the ACT from *P. haemolytica* A2, for the studied couples of substrates, and affinities of different cytidyl nucleotides to different forms of the enzyme

$K_{i\ X \to Y}$ is the association constant of the X cytidyl derivative to the Y form of the enzyme (±S.E.M.). Abbreviation: ME, methyl ester.

(a)

Parameter	Substrate A ... / Substrate B ...	Value						
		CTP Neu5Ac	CTP Neu5Ac ME	CTP Neu5Gc	CDP Neu5Ac	UTP Neu5Ac	UDP Neu5Ac	TTP Neu5Ac
K_{mA} (mM)		1.77 ± 0.16	2.6 ± 0.8	0.36 ± 0.06	2.1 ± 0.4	2.7 ± 0.3	3.0 ± 0.7	8.1 ± 0.4
K_{mB} (mM)		1.82 ± 0.20	1.3 ± 0.5	3.0 ± 0.5	1.8 ± 0.4	1.9 ± 0.3	1.9 ± 0.5	1.6 ± 0.1
V_{max} (μmol/min)		197 ± 29	219 ± 10	102 ± 7	28 ± 3	18 ± 3	5.9 ± 2.3	83 ± 25
K_{ia}		0.132 ± 0.02						
K_{ib}		0.090 ± 0.02						
K_{ip}		30.4 ± 5.3						
K_{iq}		26.43 ± 5.1						

(b)

Parameter	Inhibitor ...	Value			
		CTP	CDP	CMP	Cytidine
$K_{i\ X \to F}$		0.112 ± 0.03	0.067 ± 0.03	0.029 ± 0.01	0.013 ± 0.005
$K_{i\ X \to [FB+EQ]}$		0.079 ± 0.012	0.046 ± 0.02	0.027 ± 0.007	0.019 ± 0.005
$K_{i\ X \to E}$		7.58 ± 0.91	0.070 ± 0.02	0.019 ± 0.005	

On this basis, the experimental data were fitted to four families of Bi Bi models. There are no differences in the equations that describe the mechanisms grouped under the same family in the absence of products. The families, along with the appropriate equations, are given in the Appendix.

The residual sum of squares (Table 3) indicated that the best fit corresponded to family A ($P < 0.01$). Thus the ACT from *P. haemolytica* A2 proceeds through a Bi Bi Ping Pong mechanism, where CTP is the first substrate and CMP-NeuAc is the last product. This order in substrate addition is the same as that described for the ACT from *H. ducreyi*, although this enzyme has been shown to display an ordered Bi Bi reaction pattern [30]. It is important to stress that the identification of CTP as the first substrate was deduced from the data obtained in the absence of products. This result is due to the breakdown in the inner symmetry inherent to the Ping Pong systems, due to the asymmetric substrate inhibition.

The proposed Bi Bi Ping Pong mechanism involves a transient change in the enzyme, since CMP is linked to it after the catalytic cleavage of PP_i. An indirect observation in this sense has been reported for ACT from rat liver, for which the binding of CTP induces a conformational change that increases enzyme susceptibility to temperature [25]. Moreover, the crystal structure of ACT from *N. meningitidis* has been reported in both the absence and the presence of CDP. The binding of the substrate analogue to the enzyme is accompanied by a conformational change in a phosphate-binding loop of the protein [31]. This supports the proposed reaction sequence, which is the same for the reported Bi Bi ordered mechanism [30] and for the Bi Bi Ping Pong mechanism that we propose.

The optimal fit also yielded values for $K_{m,CTP}$ and $K_{m,NeuAc}$. Values for the substrate inhibition constants were also obtained, but analysis of the product-inhibition data was necessary for their proper definition. The K_m values were 1.77 mM for CTP and 1.82 mM for NeuAc. These results are comparable with those of the apparent K_m values for other ACTs from other sources (Table 1). The case of ACT from *H. ducreyi* is different, since this is the only ACT whose kinetics and mechanism have been properly reported. In this case $K_{m,CTP}$ is much lower: 0.010 mM. However, it is important to bear in mind that all reported values are apparent and not true K_m values, and the corresponding values cannot be contrasted in depth. Furthermore, the K_m values for ordered and Bi Bi Ping Pong models are given by a different definition, as follows:

$$K_{mA\ Ordered} = \frac{k_3 k_4}{k_1(k_3 + k_4)} \qquad K_{mB\ Ordered} = \frac{k_4(k_{-2} + k_3)}{k_2(k_3 + k_4)}$$

$$K_{mA\ Ping\ Pong} = \frac{k_4(k_{-1} + k_2)}{k_1(k_2 + k_4)} \qquad K_{mB\ Ping\ Pong} = \frac{k_2(k_{-3} + k_4)}{k_3(k_2 + k_4)}$$

In all cases k_i and k_{-i} symbolise the reaction rate coefficient of the *i*-th step of the reaction in the forward and in the reverse sense respectively. A comparison between true affinities in different mechanisms must therefore refer to true individual dissociation constants, i.e. $K_{iA} = k_{-1}/k_1$, which have the same definition in both models. Such a comparison for the ACTs is given below.

Product-inhibition data

The three kinetic models involved in family A became discernible when product inhibition was studied. Choice among rival models was carried out using PP_i as an inhibitor, owing to the simplicity and accuracy of the colorimetric method of CMP-NeuAc detection.

Three candidate models were tested, grouped in the absence of products as family A (see the Appendix):

(i) Hybrid Ping Pong Theorell–Chance, inhibited by A on both F and [FB + EQ]

(ii) Ping Pong inhibited by A on both F and [FB + EQ]

(iii) Ping Pong inhibited by A in [EA + FP] and F

The residual sum of squares (Table 3) indicated that the second model gave the best fit ($P < 0.01$). It is noteworthy that it is possible to identify the actual enzyme form that is inhibited,

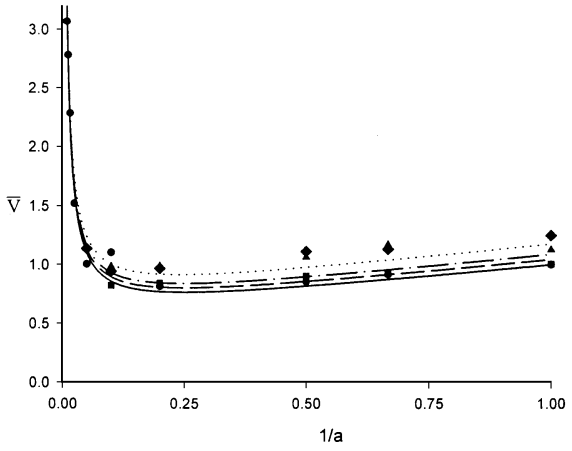

Figure 2 Plot of $\overline{V}_{a,b}$ versus 1/*a* in the presence of PP_i for the ACT from *P. haemolytica* A2$^{b=1}$

Concentration of PP_i was varied: 1 mM (●, continuous line), 2.5 mM (■, broken line), 5 mM (▲, dash-dotted line) and 10 mM (◆, dotted line). The reference concentration was 0.5 mM for both substrates. Each point represents the mean result for three experiments. Maximum S.D. was 23%. Lines were generated using constants obtained from non-linear fit of the data to eqn (A2), for a Bi Bi Ping Pong system inhibited by substrate A (CTP) in the forms F and [FB + EQ] of the enzyme, in the presence of P.

since either form provides different terms in the product-inhibition rate equation. From this fit, the values for $K_{i}^{A \rightarrow F}$ and $K_{i}^{A \rightarrow FB}$ are worked out (Table 4). The results for the $b = 1$ experimental series are given in Figure 2.

The value for K_{iA} in the ACT from *H. ducreyi*, seen to follow an ordered mechanism, was 0.046 mM [30], and the value for the enzyme from *P. haemolytica* A2, seen to follow a Ping Pong mechanism, was 0.132 mM; i.e. only three times higher. However, the values for the respective $K_{m,CTP}$ values differed by two-fold: 0.0106 mM (ACT from *H. ducreyi*) and 1.77 mM (ACT from *P. haemolytica* A2). This again emphasizes the fact that direct comparison between the K_m values actually refers to a comparison between combinations of elementary rate constants. Therefore it should not be assumed that the value of K_m describes simple enzyme–substrate affinity.

The experimental data in the presence of Q afforded results from which it was possible to obtain a complete description of the relationship between enzyme, substrates and products. All the particular dissociation constants are defined and given in Table 4. All equilibria are displaced towards CMP-NeuAc formation, with the exception of the addition of NeuAc to the active enzyme form F. This step appears to be the limiting stage of the reaction. By contrast, the limiting step in the ACT from *H. ducreyi* is the dissociation of CMP-NeuAc from the enzyme [30]. The increase in the lifetime of the reaction intermediate F in the enzyme from *P. haemolytica* A2 will be important for the regulation of the enzyme activity.

Alternative substrates

CDP, UTP, UDP and TTP were substrates for ACT activity from *P. haemolytica* A2. The corresponding K_{mA} values are similar to $K_{m,CTP}$, only the $K_{m,TTP}$ being higher (Table 4). However, V_{max} values were significantly lower for all nucleotides tested, as compared with the physiological values. Thus all the pyrimidine nucleotides seem to enter the active site of the enzyme, but only CTP efficiently yields the product NMP-NeuAc.

The experimental data corresponding to CDP were fitted to the four proposed models, as was done with the physiological substrates. The best fit also corresponded to a Bi Bi Ping Pong mechanism inhibited by substrate in two forms of the enzyme (Table 3). No substrate inhibition was detected when UTP, UDP or TTP were used as substrates. In these cases, only classic Bi Bi ordered and Ping Pong mechanisms were fitted. The best fit corresponded to the Bi Bi Ping Pong model (Table 3).

Only UTP has previously been described as a substrate for ACT activity in the mammalian enzyme, yielding about 7% of the physiological activity [34]. Previous work detected no ACT activity when CDP or TTP were used as substrates for the enzyme from rat liver [25] and from *N. meningitidis* [16]. The broad spectrum of catalytically active substrates in the ACT from *P. haemolytica* A2 has no comparison with either bacterial or animal enzymes [44].

NeuGc and NeuAc methyl ester were substrates for ACT activity, with similar values for $K_{m,NeuAc}$, $K_{m,NeuGc}$ and $K_{m,NeuAc\ methyl\ ester}$ (Table 4). The experimental data were fitted to

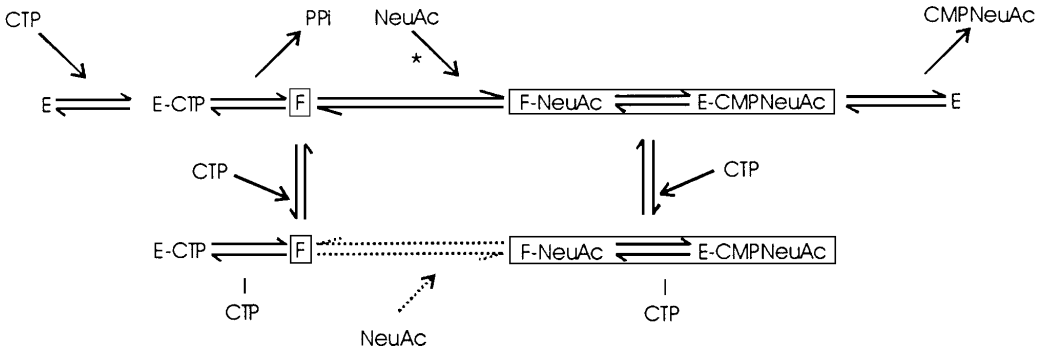

Scheme 1 Proposed Ping Pong mechanism for the ACT from *P. haemolytica* A2

The rate-limiting step of the activity (marked with an asterisk, *) is the addition of the second substrate, NeuAc, to the activated form of the enzyme. The pirimidine nucleotides CDP, UTP, UDP and TTP could substitute for CTP in the reaction. The derivatives of neuraminic acid, NeuGc and NeuAc methyl ester, could substitute for NeuAc in the reaction. The substrate CTP acts also as an inhibitor of the activity through binding to the F and [FB + EQ] forms of the enzyme. Boxes enclose the enzyme forms amenable to being captured by the inhibitor CTP. Dotted lines indicate the proposed binding of the second substrate to the inhibited form F.

Table 5 Election of the kinetic mechanism of the ACT

Data correspond to residual sum of squares in the absence of products and in the presence of the substrate analogues CMP and cytidine or in the presence of the effector UDP-GlcNAc. Mechanisms are described in the text. Each value is the mean for four experiments.

					Competitive inhibition/ prevention of regulatory inhibition						
		Competitive inhibition	Regulatory inhibition	Competitive/regulatory inhibition		Competitive inhibition	Competitive inhibition and substrate inhibition	Inhibition on [FB + EQ]	Inhibition on F	Inhibition on F and [FB + EQ]	
Effector	Number of parameters …	5	6	7	7	5	6	5	5	6	Number of data
CMP		9.497	9.401	4.218	9.023						78
Cytidine		8.689	6.545	4.009	5.605						75
UDP-GlcNAc						10.034	9.185	9.820	11.235	9.179	79

the four proposed models, and the best fit corresponded to a Bi Bi Ping Pong mechanism inhibited by substrate A on two forms of the enzyme (Table 3). According to the definitions of K_{mA} and K_{mB}, we propose the following order in the velocity constants of the binding of the second substrate: $k_{3,\text{NeuGc}} < k_{3,\text{NeuAc}} < k_{3,\text{NeuAc methyl ester}}$; and in the velocity constants of the release of the second product: $k_{4,\text{NeuAc}} < k_{4\text{NeuAc methyl ester}} < k_{4,\text{NeuGc}}$. That is, the ester derivative is a better substrate of ACT activity because it increases the efficiency of the rate-limiting step. By contrast, NeuGc is a poorer substrate, since its incorporation into the reaction sequence is less efficient. This explanation also correlates with variations in V_{max} values as follows: $V_{\text{max,NeuAc methyl ester}} > V_{\text{max,NeuAc}} > V_{\text{max,NeuGc}}$.

Activation of NeuGc into CMP-NeuGc is a classic feature of mammalian sialic acid metabolism [44]. Only *H. ducreyi* has been shown to activate NeuGc, despite the absence of this molecule in its structures [30]. Neither *E. coli* nor *N. meningitidis*, micro-organisms that synthesize a capsule of polysialic acid, use NeuGc as a substrate of ACT activity [44]. Hence *P. haemolytica* A2 is the only polysialic acid producer able to activate NeuGc into CMP-NeuGc. This is reminiscent of the animal origin of the sialic acid metabolism. Moreover, *P. haemolytica* produces an extracellular neuraminidase that hydrolyses sialic acids from macromolecules of the host [45]. The ability of activating this monomer correlates with the presence of a transporter for sialic acids in *P. haemolytica* A2 (S. Solana, I. G. Bravo, A. Reglero, L. B. Rodríguez-Aparicio, H. Martínez-Blanco and M. A. Ferrero, unpublished work).

Substrate inhibition

ACT from *P. haemolytica* A2 was inhibited by the substrate CTP. This behaviour has also been described for the enzyme from rat liver and from bovine tissues [25,46]. The best fit ($P < 0.01$) in our experiments corresponded to a model in which CTP binds to the enzyme intermediate of reaction F and to the catalytic complex [FB + EQ]. The value for $K_{i_{A \to F}}$ is the true constant of the equilibrium:

$$F + A \leftrightarrow F \cdot A$$

The value for $K_{i_{A \to [FB+EQ]}}$ is the true constant of the equilibrium:

$$[FB + EQ] + A \leftrightarrow [FB + EQ] \cdot A$$

Although we describe the binding of CTP to two forms of the enzyme, this does not imply the existence of two distinct CTP-binding regulatory sites and does not exclude the binding of NeuAc to the FA form. The true value for $K_{i_{A \to [FB+EQ]}}$ is similar to that of $K_{i_{A \to F}}$. This suggests that the true inhibitory mechanism could be of the non-competitive type (Scheme 1).

CMP and cytidine, analogues of the substrate CTP, were tested as inhibitors of ACT activity over a wide range of substrate concentrations (see the Materials and methods section). The kinetic model yielding the best fit considered the analogue as both a competitive inhibitor with respect to the catalytic site and an inhibitor by binding to the regulatory site ($P < 0.05$) (Table 5). The dissociation constants for the particular cases are given in Table 4. The affinity of cytidyl derivatives for the regulatory site showed a direct dependence on the length of the phosphate tail. Hence, CTP exhibits an affinity 1-fold higher than that of cytidine. The same effect was seen as regards the active site, CTP showing an affinity almost 3-fold higher than that of cytidine.

CTP has been described as an inhibitor of ACT activity in the rat liver enzyme, and CDP, UTP and TTP have been defined as competitive inhibitors of ACT activity [25]. In addition, ACT is

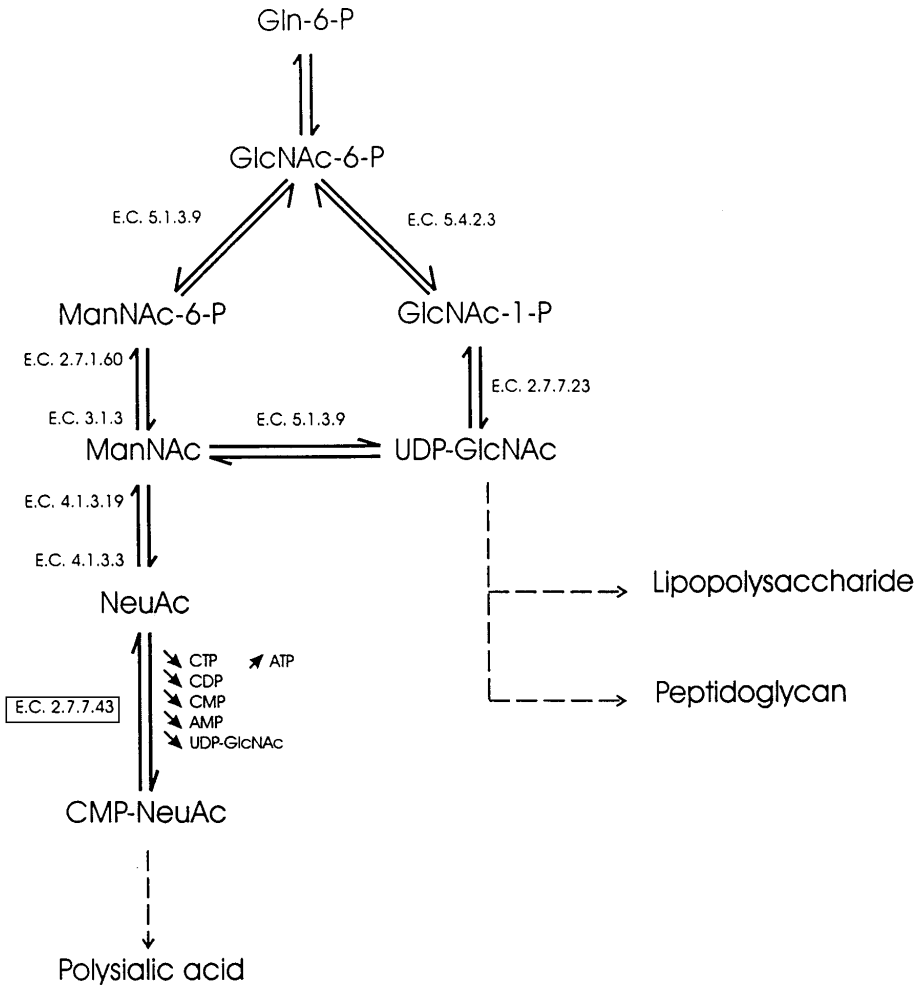

Scheme 2 Biosynthetic pathway of amino-sugar polymers in encapsulated bacteria

CMP-NeuAc is the activated monomer for incorporating into polysialic acid. UDP-GlcNAc is the activated monomer for synthesis of lipopolysaccharide and peptidoglycan. Both compete for the pool of amino-sugars. CTP, CDP, CMP, AMP and UDP-GlcNAc are inhibitors of ACT from *P. haemolytica* A2. ATP is an activator of this activity. The box encloses the EC number of the ACT activity.

competitively inhibited by CMP [25,44], and this regulation has been considered of physiological significance in mammalian sialic acid metabolism [47]. Our results show that this control is also present in a bacterial enzyme, and that the true action of CMP on ACT activity occurs through both competition for the active site and binding to the regulatory site. However, the affinity data suggest that the genuine effector on this regulatory site is the actual substrate CTP. The absence of substrate inhibition for non-cytidyl pyrimidine nucleotides points to the high specificity of this mechanism. Moreover, the regulatory site discriminates between nucleotides that are not discerned by the catalytic site.

Regulation of the ACT activity by other molecules

In bacteria, the biosynthesis of NeuAc occurs through condensation of ManNAc with either Pyr or PEP, in an overall reaction favouring ManNAc [48]. Thus extracellular NeuAc is driven into amino-sugar metabolism through its conversion into ManNAc [49]. Moreover, the pool of amino-sugars is shared by peptidoglycan, mucopolysaccharide and, in *P. haemolytica* A2, polysialic acid building systems (Scheme 2). ACT activity thus commits NeuAc to the biosynthesis of polysialic acid, since CMP-NeuAc is a substrate only for assembly into the polymer. The importance of the metabolic control of this enzyme is therefore obvious, especially since the equilibrium of the reaction lies in the direction of synthesis, in contrast with other known pyrophosphorylases [47,50]. Accordingly, we studied the effect of the key intermediate UDP-GlcNAc (Scheme 2) on ACT activity. The experimental data revealed the best fit for a model ($P < 0.05$) in which UDP-GlcNAc inhibits ACT activity through binding as an analogue of the product CMP-NeuAc, yielding a enzyme-analogue form amenable to being captured by the inhibitor CTP (Scheme 1). Thus a physiological concentration of UDP-GlcNAc inhibited ACT activity by up to 25%, suggesting the existence of cross-regulation between the amino-sugar pathways.

No ACT activity was detected when purine nucleotides were used as substrate. In contrast, ATP, GTP, AMP and GMP regulated the enzyme activity in a concentration-dependent fashion (Table 6). These nucleotides significantly inhibited the enzyme when assayed at above 5.0 mM, this value being the highest intracellular concentration reported for these molecules

Table 6 Mean effect of the presence of ATP, AMP, GTP, GMP, CMP, cytidine and UDP-GlcNAc on the ACT from *P. haemolytica* A2, across a wide range of substrate concentrations

Each value represents the mean for four experiments. The number in parentheses represents the number of values used in calculating the mean.

Nucleotide (concn. in mM)	Activity (%, mean ± S.E.M.)
ATP	
10	40.0 ± 0.8 (20)
5.0	98.8 ± 1.7 (19)
1.0	119.8 ± 2.1 (21)
AMP	
10	35.5 ± 1.4 (19)
5.0	69.7 ± 1.8 (21)
1.0	82.7 ± 1.7 (21)
CMP	
50	41.6 ± 0.8 (15)
20	60.0 ± 0.2 (15)
10	67.3 ± 0.8 (21)
5.0	73.0 ± 0.8 (22)
UDP-GlcNAc	
10	74.1 ± 0.5 (14)
5.0	76.1 ± 0.6 (20)
1.0	83.0 ± 0.6 (18)
GTP	
10	61.1 ± 1.3 (21)
1.0	98.6 ± 2.0 (21)
GMP	
20	36.4 ± 2.0 (18)
10	40.5 ± 1.1 (19)
5.0	62.9 ± 1.4 (21)
1.0	98.8 ± 2.3 (21)
Cytidine	
60	63.3 ± 0.9 (14)
40	62.8 ± 1.0 (15)
20	61.4 ± 0.8 (15)
10	74.4 ± 0.6 (14)
5.0	76.4 ± 0.8 (15)

[51]. Each nucleotide was tested as an effector over a wide range of substrate concentrations (see the Materials and methods section); thus the inhibition value given is significant for both low and high substrate concentrations. At the physiological level, considered as 1.0 mM, neither GTP nor GMP affected the enzyme activity. By contrast, ATP activated the enzyme by 20 %, and AMP inhibited the activity by 20 %. Thus fine regulation of ACT activity could respond to the ATP/AMP ratio, which reflects the energy charge of the cell.

The characteristics of ACTs make it difficult to clearly differentiate between the properties of ACT in mammals and in bacteria, and between the properties of small and large ACTs [30]. All ACTs aggregate when are purified, whether natively or as a result of purification process, and the crystallized enzyme forms a dimer [31]. The ACTs from mammalian sources and from *E. coli* and *P. haemolytica* A2 are large enzymes with twice the molecular mass of those reported for the monomers of the small ACTs from *H. ducreyi* and *N. meningitidis* [16,19,24]. These two small bacterial enzymes also display the lowest K_m values for both substrates, while large bacterial and mammalian enzymes have comparable K_m values. The kinetic behaviour has previously been elucidated for ACT from *H. ducreyi*, seen to be an ordered Bi Bi enzyme [30]. Here we summarize the kinetic description of the ACT from *P. haemolytica* A2, which is a Bi Bi Ping Pong enzyme. Additionally, mammalian enzymes have been shown to utilize NeuGc as substrate and only the *H. ducreyi* protein, a small bacterial enzyme, and that of *P. haemolytica* A2, a large bacterial enzyme, also catalyse the formation of CMP-NeuGc, thus complicating the relationship pattern along the whole group. In this sense, elucidation of the kinetic mechanisms of mammalian ACTs together with crystallization studies will hopefully shed light on this unclear evolutionary divergence and/or convergence process.

This work was supported by the Dirección General de Investigación Científica y Técnica (PB96-0161). I. G. B. is the recipient of a Fundación Ramón Areces Postgraduate Scholarship.

APPENDIX

Data analysis

Data analysis in the absence of products

All experimental data were fitted to the corresponding equations derived from the normalized plot premises (see the accompanying paper [37a]) by non-linear regression analysis using SigmaPlot software (Jandel), and the nomenclature of Cleland.

Initial-velocity data were fitted to three different equations, corresponding to different families of Bi Bi mechanisms:

Family A (eqn A1)

(i) Hybrid Ping Pong Theorell–Chance, inhibited by substrate A on F and on [FB + EQ]

(ii) Ping Pong inhibited by substrate A on F and [FB + EQ]

(iii) Ping Pong inhibited by substrate A on [EA + FP] and F

$$\bar{V}_{\substack{a,b \\ A\rightarrow(\text{two forms})}} = \frac{K_{mB}aA + K_{mA}bB + aAbB + K_{mB}\,K_{i}\,{}_{A\rightarrow F}\,a^2A^2 + K_{r}\,{}_{A\rightarrow\left[\begin{smallmatrix}EA+FP\\ \text{or}\\ FB+EQ\end{smallmatrix}\right]}\,K_{i}\,a^2bA^2B}{ab\cdot den}$$

Family B

(i) Hybrid Ping Pong Theorell–Chance, inhibited by substrate A on [FB + EQ]

(ii) Ping Pong inhibited by substrate A on [FB + EQ]

(iii) Ping Pong inhibited by substrate A on [EA + FP]

$$\bar{V}_{\substack{a,b \\ A\rightarrow(\text{one form})}} = \frac{K_{mB}aA + K_{mA}bB + aAbB + K_r \underset{A\rightarrow\left[\begin{smallmatrix}EA+FP\\ or\\ FB+EQ\end{smallmatrix}\right]}{K_i} a^2bA^2B}{ab\cdot den}$$

Family C

(i) Ordered inhibited by substrate A on [EAB + EPQ]

(ii) Ordered inhibited by substrate A on [EQ]

(iii) Ordered inhibited by substrate A on [EAB + EPQ] and [EQ]

$$\bar{V}_{\substack{a,b \\ A\rightarrow(\text{two forms})}} = \frac{K_{iA}K_{mB} + K_{mB}aA + K_{mA}bB + aAbB + K_{mB}\underset{A\rightarrow F}{K_i}\, a^2A^2 + K_r \underset{A\rightarrow\left[\begin{smallmatrix}EA+FP\\ or\\ FB+EQ\end{smallmatrix}\right]}{K_i} a^2bA^2B}{ab\cdot den}$$

Family D

(i) Ordered inhibited by substrate A on EA and EAB

$$\bar{V}_{\substack{a,b \\ A\rightarrow(\text{one form})}} = \frac{K_{iA}K_{mB} + K_{mB}aA + K_{mA}bB + aAbB + K_r \underset{A\rightarrow\left[\begin{smallmatrix}EA\\ and\\ EAB\end{smallmatrix}\right]}{K_i} a^2bA^2B}{ab\cdot den}$$

In all cases $\bar{V}_{a,b}$ is the normalized velocity in the presence of a times and b times the reference concentration for substrates A and B respectively; K_{mX} is the Michaelis constant for the designated substrate X; K_{iX} is the dissociation constant for the substrate X, and $\underset{A\rightarrow X}{K_i}$ is the formation constant of the substrate A–enzyme form X complex, and K_r is defined as $K_r = k_2/(k_2 + k_4)$, where k_i and k_{-i} symbolize the reaction rate coefficient of the i-th step of the reaction in the forward and in the reverse sense respectively.

Data analysis: presence of products

The data obtained in the presence of PP_i were fitted to three different Ping Pong mechanisms with two substrate inhibition targets:

(i) Hybrid Bi Bi Ping Pong Theorell–Chance mechanism, inhibited by substrate A on F and [FB + EQ]

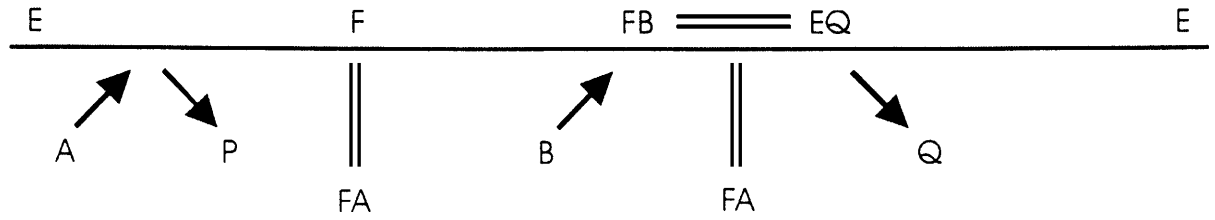

$$\bar{V}_{\substack{a,b \\ P\neq 0}} = \frac{K_{mB}aA + K_{mA}bB + aAbB + K_{mB}\underset{A\rightarrow F}{K_i}\, a^2A^2 + K_r \underset{A\rightarrow FB}{K_i}\, a^2bA^2B + \dfrac{K_{mB}}{K_{iA}}P}{ab\cdot den}$$

(ii) Bi Bi Ping Pong mechanism, inhibited by substrate A on F and [FB + EQ] (eqn A2)

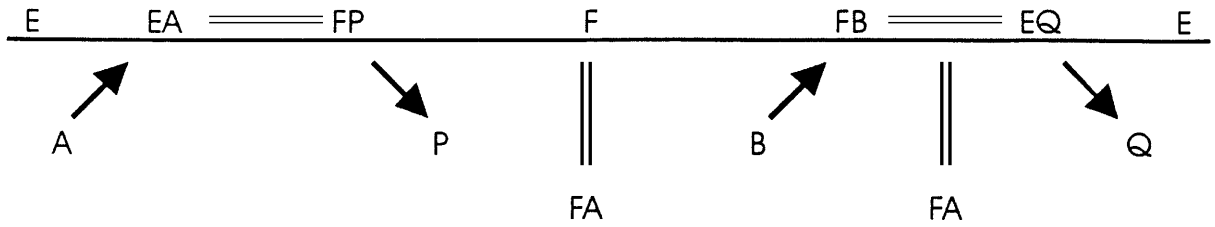

$$\bar{V}_{\substack{a,b \\ P\neq 0}} = \frac{K_{mB}aA + K_{mA}bB + aAbB + K_{mB}\underset{A\rightarrow F}{K_i}\, a^2A^2 + K_r \underset{A\rightarrow FB}{K_i}\, a^2bA^2B + \dfrac{K_{mB}}{K_{iP}}aAP + \dfrac{K_{mB}K_{iA}}{K_{iP}}P}{ab\cdot den}$$

(iii) Bi Bi Ping Pong mechanism inhibited by substrate A on [EA + FP] and F

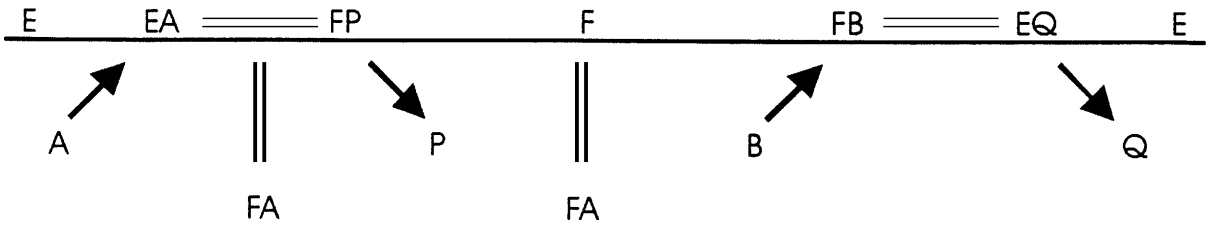

$$\bar{V}_{\substack{a,b \\ P\neq 0}} = \frac{K_{mB}aA + K_{mA}bB + aAbB + K_{mB}\underset{A\to F}{K_i}\,a^2A^2 + K_r\underset{A\to EA}{K_i}\,a^2bA^2B + \frac{K_{mQ}K_{mA}K_{iB}}{K_{mP}K_{iQ}}P + K_{mA}K_{iP}aAP + K_{mB}\underset{A\to EA}{K_i}\,a^2A^2P}{ab\cdot den}$$

The data obtained in the presence of CMP-NeuAc were fitted to the corresponding equation of a Bi Bi Ping Pong mechanism inhibited by substrate A on F and [FB + EQ]:

$$\bar{V}_{\substack{a,b \\ P\neq 0}} = \frac{K_{mB}aA + K_{mA}bB + aAbB + K_{mB}\underset{A\to F}{K_i}\,a^2A^2 + K_r\underset{A\to FB}{K_i}\,a^2bA^2B + \frac{K_{mA}K_{iB}}{K_{iQ}}Q + \frac{K_{mA}}{K_{iQ}}bBQ + \underset{A\to FB}{K_i}\,\frac{K_{mA}K_{iB}}{K_{iQ}}aAQ + \underset{A\to F}{K_i}\,K_{mA}abABQ}{ab\cdot den}$$

Data analysis: analogues of CTP

The experimental data were fitted to four different equations corresponding to the four situations considered. In all cases, the basic equation was modified by the addition of terms to the numerator. This basic equation, a Bi Bi Ping Pong system in the absence of products, with substrate A acting as an inhibitor on F and on [FB + EQ], was:

$$\bar{V}_{a,b} = \frac{K_{mA}bB + aAbB + K_{mB}\underset{A\to F}{K_i}\,a^2A^2 + K_r\underset{A\to FB}{K_i}\,a^2bA^2B}{ab\cdot den}$$

(i) The analogue competes with CTP for the catalytic site only; the new term is:

$$K_{mA}\underset{I\to E}{K_i}\,bBI$$

(ii) The analogue competes with CTP for the regulatory site/s, and binding to the regulatory sites inhibits the activity; the new terms are:

$$K_{mB}\underset{I\to F}{K_i}\,aAI + K_r\underset{I\to FB}{K_i}\,abABI$$

(iii) the analogue competes with CTP for both, the catalytic and the regulatory site/s, and binding to the regulatory sites inhibits the activity; the new terms are:

$$K_{mA}\underset{I\to E}{K_i}\,bBI + K_{mB}\underset{I\to F}{K_i}\,aAI + K_r\underset{I\to FB}{K_i}\,abABI$$

(iv) the analogue competes with CTP for both the catalytic and the regulatory site/s, and binding to the regulatory sites does not inhibit the activity; the overall equation becomes:

$$\bar{V}_{a,b} = \frac{K_{mB}aA\left(1 + \frac{\underset{A\to F}{K_i}\,aA}{1 + \underset{I\to F}{K_i}\,I}\right) + K_{mA}bB\left(1 + \underset{I\to E}{K_i}\,I\right) + aAbB\left(1 + \frac{\underset{A\to FB}{K_i}\,K_raA}{1 + \underset{I\to FB}{K_i}\,I}\right)}{ab\cdot den}$$

where $\underset{I\to X}{K_i}$ is the association constant of the inhibitor to the X form of the enzyme.

Data analysis: presence of UDP-GlcNAc

The experimental data were fitted to five equations, corresponding to the four situations considered, as follows:

(i) UDP-GlcNAc is a competitive inhibitor, an analogue of CMP-NeuAc; the new term in the numerator of the equation is:

$$K_{mA}\underset{I\to E}{K_i}\,bBI$$

(ii) UDP-GlcNAc is a competitive inhibitor, an analogue of CMP-NeuAc, and CTP binds, as an inhibitor, to the form EI; the new terms are:

$$\underset{I \to E}{K_{mA}}\ \underset{I \to E}{K_i}\ bBI + \underset{A \to FB}{K_r}\ \underset{A \to FB}{K_i}\quad \underset{I \to E}{K_i}\ a^2bA^2B$$

(iii) UDP-GlcNAc is an inhibitor that binds the [FB+EQ] form of the enzyme; the new term is:

$$\underset{I \to FB}{K_i}\ abABI$$

(iv) UDP-GlcNAc is an inhibitor that binds the F form of the enzyme; the new term is:

$$\underset{I \to FB}{K_{mB}}\ \underset{I \to FB}{K_i}\ aAI$$

(ii) UDP-GlcNAc is an inhibitor that binds the F form and the [FB+EQ] form of the enzyme; the new terms are:

$$\underset{I \to FB}{K_{mB}}\ \underset{I \to FB}{K_i}\ aAI + \underset{I \to FB}{K_i}\ abABI$$

Data analysis: choice among rival kinetic models

For choice of the best fit between models with different numbers of parameters we followed the criteria of Mannervik [52]. The rival models tested are expressed as normalized equations that differ in the addition of terms to a simpler expression. Introduction of the additional parameters is commonly accompanied by a decrease in the residual sum of squares. The question consists of deciding whether this difference is large enough to ensure acceptance of the complex model instead of the simpler one. The significance of the improvement obtained by the addition of the new parameters is tested by comparing the quotient

$$\frac{(SS_j - SS_k)(n - p_k)}{(p_j - p_k)SS_k}$$

with the F statistic, $F_{pk-pj,\ n-pk}$ at the desired level of probability. SS_j is the residual sum of the simpler model, with p_j parameters; SS_k is the residual sum of the complex model, with p_k parameters; n is the number of data.

REFERENCES

1 Smith, G. R. (1961) The characteristics of two types of *Pasteurella haemolytica* associated with different pathological conditions in sheep. J. Pathol. Bacteriol. **81**, 431–440

2 Biberstein, E. L., Gills, M. and Knight, H. (1960) Serological types of *Pasteurella haemolytica*. Cornell Vet. **50**, 283–300

3 Biberstein, E. L. and Francis, C. K. (1968) Nucleic acid homologies between the A and T types of *Pasteurella haemolytica*. J. Med. Microbiol. **1**, 105–108

4 Adlam, C. and Rutter, J. M. (1989) *Pasteurella* and Pasteurellosis, Academic Press, London

5 Adlam, C., Knight, J. M., Mugridge, A., Williams, J. M. and Lindon, J. C. (1987) Production of colominic acid by *Pasteurella haemolytica* serotype A2 organisms. FEBS Microbiol. Lett. **42**, 23–25

6 Barry, G. T. (1959) Detection of sialic acid in various *E. coli* strains and other species of bacteria. Nature (London) **183**, 117–118

7 Masson, L. and Holbein, B. E. (1983) Physiology of sialic acid capsular polysaccharide synthesis in serogroup B of *N. meningitidis*. J. Bacteriol. **54**, 728–736

8 Silver, R. P. and Vimr, E. R. (1990) Polysialic acid capsule of *Escherichia coli* K1. In The Bacteria, vol. 11: Molecular Basis of Bacterial Pathogenesis (Iglewsky, B. and Miller, V., eds.), pp. 39–60, Academic Press, New York

9 Bayer, M. E. and Bayer, M. H. (1994) Biophysical and structural aspects of the bacterial capsule. ASM News **60**, 192–198

10 Vimr, E., Steenbergen, S. and Cieslewicz, (1995) Biosynthesis of the polysialic acid capsule in *Escherichia coli* K1. J. Ind. Microbiol. **15**, 352–360

11 Rodríguez-Aparicio, L. B., Ferrero, M. A., Revilla-Nuin, B., Martínez-Blanco, H. and Reglero, A. (1999) Determination of different amino sugar 2′-epimerase activities by coupling to *N*-acetylneuraminate synthesis. Biochim. Biophys. Acta **1428**, 305–313

12 Swartley, J. S. and Stephens, D. S. (1994) Identification of a genetic locus involved in the biosynthesis of *N*-acetyl-D-mannosamine, a precursor of the ($\alpha 2 \rightarrow 8$)-linked polysialic acid capsule of serogroup B *Neisseria meningitidis*. J. Bacteriol. **176**, 1530–1534

13 Gosh, S. and Roseman, S. (1965) The sialic acids. *N*-Acetylglucosamine-6-P 2-epimerase. J. Biol. Chem. **240**, 1525–1530

14 Vann, W. F., Tavarez, J. J., Crowley, J., Vimr, E. and Silver, R. P. (1997) Purification and characterization of the *Escherichia coli* K1 *neuB* gene product *N*-acetylneuraminic acid synthetase. Glycobiology **7**, 697–701

15 Rodríguez-Aparicio, L. B., Ferrero, M. A. and Reglero, A. (1995) *N*-Acetyl-D-neuraminic acid synthesis in *Escherichia coli* K1 occurs through condensation of *N*-acetyl-D-mannosamine and pyruvate. Biochem. J. **308**, 501–505

16 Warren, L. and Blacklow, R. S. (1962) The biosynthesis of cytidine 5′-monophospho-*N*-acetylneuraminic acid by an enzyme from *N. meningitidis*. J. Biol. Chem. **237**, 3527–3534

17 Ferrero, M. A., Reglero, A., Fernandez-Lopez, M., Ordas, R. and Rodriguez-Aparicio, L. B. (1996) *N*-Acetyl-D-neuraminic acid lyase generates the sialic acid for colominic acid biosynthesis in *Escherichia coli* K1. Biochem. J. **317**, 157–165

18 Schauer, R. (1982) Chemistry, metabolism and biological functions of sialic acids. Adv. Carbohydr. Chem. Biochem. **40**, 131–234

19 Vann, W. F., Silver, R. P., Abeijon, C., Chang, K., Aaronson, W., Sutton, A., Finn, C. W., Lindner, W. and Kotsatos, M. (1987) Purification, properties and genetic location of *Escherichia coli* cytidine 5′-monophosphate *N*-acetylneuraminic acid synthetase. J. Biol. Chem. **262**, 17556–17562

20 Zapata, G., Vann, W. F., Aaronson, L. and Moos, M. (1989) Sequence of the cloned *E. coli* K1 CMP-N-acetylneuraminic acid synthetase gene. J. Biol. Chem. **264**, 14769–14774

21 Ganguli, S., Zapata, G., Wallis, T., Reid, C., Boulnois, G., Vann, W. and Roberts, I. S. (1994) Molecular cloning and analysis of genes for sialic acid synthesis in *Neisseria meningitidis* group B and purification of the meningococcal CMP-NeuNAc synthetase enzyme. J. Bacteriol. **176**, 4593–4589

22 Haft, R. F. and Wessels, M. R. (1994) Characterization of CMP-*N*-acetylneuraminic acid synthetase of group B streptococci. J. Bacteriol. **176**, 7372–7374

23 Haft, R. F., Wessels, M. R., Mebane, M. F., Conaty, N. and Rubens, C. E. (1996) Characterization of cpsF and its product CMP-*N*-acetylneuraminic acid synthetase, a group B streptococcal enzyme that can function in K1 capsular polysaccharide biosynthesis in *Escherichia coli*. Mol. Microbiol. **19**, 555–563

24 Tullius, M. V., Munson, Jr., R. S., Wang, J. and Gibson, B. W. (1996) Purification, cloning, and expression of a cytidine 5′-monophosphate *N*-acetylneuraminic acid

synthetase from *Haemophilus ducreyi*. J. Biol. Chem. **271**, 15373–15380
25 Rodríguez-Aparicio, L. B., Luengo, J. M., González-Clemente, C. and Reglero, A. (1992) Purification and characterization of the nuclear cytidine 5′-monophosphate *N*-acetylneuraminic acid synthetase from rat liver. J. Biol. Chem. **267**, 9257–9263
26 Munster, A. K., Eckhardt, M., Potvin, B., Muhlenhoff, M., Stanley, P. and Gerardy-Schahn, R. (1998) Mammalian cytidine 5′-monophosphate *N*-acetylneuraminic acid synthetase: a nuclear protein with evolutionarily conserved structural motifs. Proc. Natl. Acad. Sci. U.S.A. **95**, 9140–9145
27 Potvin, B., Raju, T. S. and Stanley, P. (1995) lec32 is a new mutation in chinese hamster ovary cells that esentially abrogates CMP-*N*-acetylneuraminic acid synthetase activity. J. Biol. Chem. **270**, 30415–30421
28 Vionnet, J., Concepcion, N., Warner, T., Zapata, G., Hanover, J. and Vann, W. F. (1999) Purification of CMP-*N*-acetylneuraminic acid synthetase from bovine anterior pituitary glands. Glycobiology **9**, 481–487
29 Ambrose, M. G., Freese, S. J., Reinhold, M. S., Warner, T. G. and Vann, W. F. (1992) ^{13}C NMR investigation of the anomeric specificity of CMP-*N*-acetylneuraminic acid synthetase from *Escherichia coli*. Biochemistry **31**, 775–780
30 Samuels, N. M., Gibson, B. W. and Miller, S. M. (1999) Investigation of the kinetic mechanism of cytidine 5′-monophosphate *N*-acetylneuraminic acid synthetase from *Haemophilus ducreyi* with new insights on rate-limiting steps from product inhibition analysis. Biochemistry **38**, 6195–6203
31 Mosimann, S. C., Gilbert, M., Dombrovsky, D., To, R., Wakarchuk, W. and Strydnadka, N. C. J. (2001) Structure of a sialic acid activating synthetase, CMP acylneuraminate synthetase in the presence and absence of CDP. J. Biol. Chem. **276**, 8190–8196
32 Puente-Polledo, L., Reglero, A., González-Clemente, C., Rodríguez-Aparicio, L. B. and Ferrero, M. A. (1998) Biochemical conditions for the production of polysialic acid by *Pasteurella haemolytica* A2. Glycoconj. J. **15**, 855–861
33 Barrallo, S., Reglero, A., Revilla-Nuin, B., Martínez-Blanco, H., Rodríguez-Aparicio, L. B. and Ferrero, M. A. (1999) Regulation of capsular polysialic acid biosynthesis by temperature in *Pasteurella haemolytica* A2. FEBS Lett. **445**, 325–328
34 Kean, E. L. and Roseman, S. (1966) The sialic acids. X. Purification and properties of cytidine 5′-monophosphosialic acid synthetase. J. Biol. Chem. **241**, 5643–5650
35 Rodríguez-Aparicio, L. B., Reglero, A., Ortiz, A. I. and Luengo, J. M. (1988) Effect of physical and chemical conditions on the production of colominic acid by *Escherichia coli* in a defined medium. Appl. Microbiol. Biotechnol. **27**, 474–483
36 O'Brien, W. E. (1976) A continuous spectrophotometric assay for argininosuccinate synthetase based on pyrophosphate formation. Anal. Biochem. **76**, 423–430
37 Bradford, M. (1976) Rapid and sensitive method for the quantitation of microgram quantities of protein utilizing the principle of protein-dye-binding. Anal. Biochem. **72**, 248–254
37a Bravo, I. G., Busto, F., De Arriaga, D., Ferrero, M. A., Rodríguez-Aparacio, L. B., Martínez-Blanco, H. and Reglero, A. (2001) A normalized plot as a novel and time-saving tool in complex enzyme kinetic analysis. Biochem. J. **358**, 573–583

Received 16 March 2001/29 May 2001; accepted 26 June 2001

38 Shames, S. L., Simon, E. S., Christopher, C. W., Schmid, W., Whitesides, G. M. and Yang, L. L. (1991) CMP-N-acetylneuraminic acid synthetase from *E. coli*: high level expression, purification and use in the enzymatic synthesis of CMP-N-acetylneuraminic acid and CMP-neuraminic acid derivatives. Glycobiology **1**, 187–191
39 Tullius, M. V., Vann, W. F. and Gibson, B. W. (1999) Covalent modification of Lys19 in the CTP binding site of cytidine 5′-monophosphate *N*-acetylneuraminic acid synthetase. Protein Sci. **8**, 666–675
40 Stoughton, D. M., Zapata, G., Picone, R. and Vann, W. F. (1999) Identification of Arg-12 in the active site of *Escherichia coli* K1 CMP-sialic acid synthetase. Biochem. J. **343**, 397–402
41 Bork, P., Holm, L., Koonin, E. V. and Sander, C. (1995) The cytidyltransferase superfamily: identification of the nucleotide-binding site and fold prediction. Proteins **22**, 259–266
42 Ghalambor, M. A. and Heath, E. C. (1966) The biosynthesis of cell wall in lipopolysaccharide in *Escherichia coli*. IV. Purification and properties of cytidine monophosphate 3-deoxy-D-manno-octolusonate synthetase. J. Biol. Chem. **241**, 3216–3221
43 Goldman, R. C. and Kohlbrenner, W. E. (1985) Molecular cloning of the structural gene coding for CTP:CMP-3-deoxy-manno-octulosonate cytidyltransferase from *Escherichia coli* K12. J. Bacteriol. **163**, 256–261
44 Kean, E. L. (1991) Sialic acid activation. Glycobiology **1**, 441–447
45 Straus, D. C., Jolley, W. L. and Purdy, C. W. (1993) Characterization of neuraminidases produced by various serotypes of *Pasteurella haemolytica*. Infect. Inmun. **61**, 4669–4674
46 Petrie, R. C. and Korytnyk, W. (1983) A high-performance liquid chromatography method for the assay of cytidine monophosphate-sialic acid synthetase. Anal. Biochem. **131**, 153–159
47 Schauer, R. (1982) Sialic acids: Chemistry, Metabolism and Function, Springer-Verlag, New York
48 Comb, D. G. and Roseman, S. (1960) J. Biol. Chem. **235**, 2529–2537
49 Plumbridge, J. and Vimr, E. (1999) Convergent pathways for utilization of the aminosugars *N*-acetylglucosamine, *N*-acetylmannosamine, and *N*-acetylneuraminic acid by *Escherichia coli*. J. Bacteriol. **181**, 47–54
50 Gabriel, O. (1987) Biosynthesis of sugar residues for glycogen, peptidoglycan, lipopolysaccharide, and related systems in *Escherichia coli* and *Salmonella typhymurium*. In Cellular and Molecular Biology, vol. 1 (Neidhardt, F. C., ed.), pp. 504–511, American Society for Microbiology, New York
51 Karl, D. M. (1980) Cellular nucleotide measurements and applications in microbial ecology. Microbiol. Rev. **44**, 739–796
52 Mannervik, B. (1982) Regression analysis, experimental error and statistical criteria in the design and analysis of experiments for discrimination between rival kinetic models. Methods Enzymol. **87**, 370–380